

## Conference Paper

# The Effect of Quantum Dot Shell Structure on Fluorescence Quenching By Acridine Ligand

Linkov P.A.<sup>1,2</sup>, Vokhmintcev K.V.<sup>1</sup>, Samokhvalov P.S.<sup>1</sup>, Laronze-Cochard M.<sup>3</sup>, Sapi J.<sup>3</sup>, and Nabiev I.R.<sup>1,2</sup>

<sup>1</sup>National Research Nuclear University MEPhI (Moscow Engineering Physics Institute), Kashirskoe shosse 31, Moscow, 115409, Russia

<sup>2</sup>Laboratoire de Recherche en Nanosciences, LRN - EA4682, and <sup>3</sup>Institut de Chimie Moléculaire de Reims, UFR de Pharmacie, Université de Reims Champagne-Ardenne, 51100 Reims, France

## Abstract

The current strategy for the development of advanced methods of tumor treatment focuses on targeted drug delivery to tumor cells. Quantum dot (QD) - semiconductor fluorescent nanocrystal, conjugated with a pharmacological ligand, such as acridine, ensures real-time tracking of the delivery process of the active substance. However, the problem of QD fluorescence quenching caused by charge transfer can arise in the case when acridine is bound to the QD. We found that QD shell structure has a defining role on photoinduced electron transfer from QD on acridine ligand which leads to quenching of QD photoluminescence. We have found that multishell CdSe/ZnS/CdS/ZnS QD structure provides minimal reduction of photoluminescence quantum yield at minimal shell thickness compared to classical thin ZnS or "giant" shells. Thus, CdSe/ZnS/CdS/ZnS core/multishell QD could be an optimal choice for engineering of small-sized acridine-based fluorescent labels for tumor diagnosis and treatment systems.

**Keywords:** Quantum dot, photoluminescence quenching, DNA ligand, acridine derivative.

## 1. Introduction

Nanotechnologies open new horizons for application of new materials in biomedicine [1–3]. The current strategy for the development of advanced methods of tumor treatment focuses on targeted drug delivery to tumor cells [2, 4, 5]. Linking a fluorescent imaging agent to a biomarker-recognizing molecule conjugated with a pharmacological agent ensures real-time tracking of the delivery process of the active substance. Quantum dots (QDs) are semiconductor fluorescent nanocrystals with unique fluorescence characteristics: size-tunable light emission, high brightness, and long-term stability of optical properties [6–8]. Thus, water-soluble QDs, stabilized with hydrophilic organic

Corresponding Author:

Linkov P.A.

valinkov@gmail.com

Received: 17 January 2018

Accepted: 25 March 2018

Published: 17 April 2018

Publishing services provided by  
Knowledge E

© Linkov P.A. et al. This article is distributed under the terms of the [Creative Commons Attribution License](#), which permits unrestricted use and redistribution provided that the original author and source are credited.

Selection and Peer-review under the responsibility of the PhysBioSymp17 Conference Committee.

 OPEN ACCESS

ligands that provide long-term stability and size monodispersity, can be used as efficient biomedical fluorescent labels for real-time delivery control [9] and tracking of the pharmacological substance [10, 11].

Heterocyclic nitrogen-containing molecules such as acridine derivatives [12] exhibit affinity to G-quadruplex - planar structures, formed by telomere single-stranded nucleotide sequences, that are rich in guanine [12, 13] at each end of a DNA, which protects the end of the chromosome from deterioration [14]. Previously it was shown that 4,5,9-trisubstituted acridine derivative was able to specifically bind to the G-quadruplex and to effectively stabilize the telomere structure [12, 15], protecting the end of the chromosome from cutting and cancerous activity. Thus, acridine derivatives can be used as pharmacological components of a multifunctional nanoprobe. Also acridine-based ligands (AL) are effective charge carrier transfer system because of their polyaromatic structure. HOMO and LUMO energy levels [16, 17] of 4,5-acridine derivatives are comparable to the ones of semiconductor nanocrystals [18], what allows to use acridine-based molecules as hole transporting material in designing of perovskite solar cells [16] and light-emitting diodes [19]. On the other hand, such a charge transfer leads to the problem of QD fluorescence quenching [20, 21] by photo-induced electron transfer (PET) [22]. This hampers the use of acridine derivatives as targeting agents in designing QD-based nanoprobe.

Here, we addressed the problem of acridine derivative conjugation to QDs from the viewpoint of the effects of inorganic shell structure and shell thickness of CdSe-based core/shell QDs on the degree of fluorescence quenching. For investigation of this phenomenon we synthesized series of CdSe-based QDs covered with different shells, varying shell material (CdS and ZnS) and shell thickness, and made a series of experiments on QD's PL quenching by excess of AL.

## 2. Materials and Methods

4,5,9-substituted acridine derivative molecule (as shown in Fig. 3) was synthesized starting from acridine by following the general procedures described in [12]. The molecule was confirmed by electrospray-MS (MSQ ThermoFinnigan apparatus) and characterized using absorbance and photoluminescence (PL) spectroscopy. Absorption and PL spectra of the obtained compound are shown in Fig. 1A.

QDs with different shell structure were synthesized by a two-step procedure: (i) synthesis of CdSe cores using the hot injection method in high temperature boiling solvent (1-octadecene), and (ii) synthesis of highly luminescent core/shell QDs by coating of

purified cores [23] with different types of shells using the SILAR approach [24, 25]. This method allows growing given number of shell layers in the layer-by-layer regime with highest possible precision. In this work CdSe QD cores were coated with different shells: three-monolayer (3-ML) thick ZnS shell, "giant" 5-ML ZnS thick shell and a "multishell" (MS) - ZnS/CdS/ZnS shell with an overall three-monolayer total thickness. The first type of QDs is a "classical" one-component wide-band gap shell. The thickness of three monolayers provides sufficient protection of the charge carriers in CdSe cores in polar media. "Giant" shell allows to suppress Auger recombination, and thus to escape large nonradiative losses and to minimize fluorescence intermittency ("blinking") from single nanocrystals [26, 27]. MS shell, as we have shown previously, provides high localization of charges inside fluorescent cores at a relatively low shell thickness [25].

Water-soluble QDs were obtained by exchange of the native hydrophobic ligands of as-prepared core/shell QDs with a mixture of SH-PEG derivatives with hydroxyl and carboxyl functional groups in ratio SH-PEG-OH / SH-PEG-COOH 0.9/0.1 respectively. Absorption and emission spectra of synthesized QD samples dispersed in phosphate buffer solution are shown in Fig. 1A.

In our experiments solutions of each type of QDs containing  $\sim 1$  nmol ( $1 \mu\text{M}$ ) of nanoparticles was titrated with 1 mg/ml stock solution of AL in 0,05 M phosphate buffer solution (pH = 8.0). The example kinetic of quenching of the CdSe/ZnS/CdS/ZnS QDs with different excess of AL is shown in Fig. 2B.

### 3. Results and Discussion

The absorption bands of AL in the wavelength region between 300 and 450 nm are considered as the  $\pi$ - $\pi$  transitions of the complex  $\pi$ -conjugated system of acridine [20]. Photoluminescence and absorption maxima of AL in aqueous solution (Fig. 2A) were observed at 417 nm and 487 nm, respectively, with a large Stokes shift of 60 nm. Water solutions of obtained QDs exhibited PL / absorbance maxima at 503/472 nm for CdSe/ZnS (3-ML), 572/551 nm for CdSe/ZnS (5-ML) and 584/563 nm for CdSe/MS (Fig. 1A). As can be seen from the presented spectra, PL full width at half maximum amounted close to 40 nm, which indicates size homogeneity of the studied QD ensembles. Presence of small quantity of carboxyl groups on the surface of QDs provides a small negative surface charge ( $\sim -10$  mV), which prevents aggregation of quantum dots. Size of QDs dispersed in 0,05 M phosphate buffer solution (pH = 8.0) was measured by dynamic light scattering using Malvern Zetasizer Nano ZS, and found to be  $\sim 10 - 12$  nm, what confirms monodispersity of QDs in solution [28].

The physical diameters of inorganic part of QDs were 4,3/7/5 nm for CdSe/ZnS (3-ML), CdSe/ZnS (5-ML) and CdSe/MS, respectively, which are calculated based on size of core and projected shell thickness using crystallographic data and detailed structural models of QDs. The diameter of CdSe core was determined from an empirical calibration function which correlates the position of the first exciton transition in the optical absorption spectrum and the size of QDs [29].

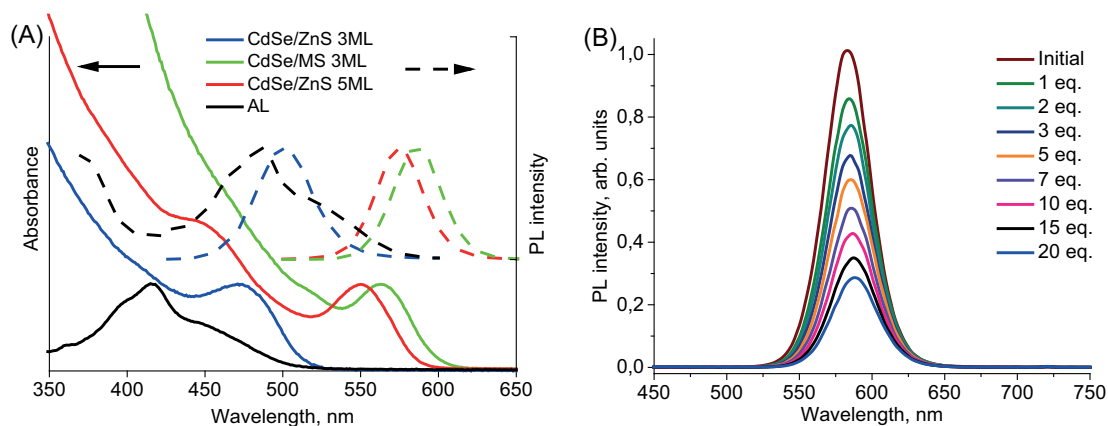


**Figure 1:** (A) Fluorescence and absorbance spectra of series of acridine ligand (AL) and highly luminescent core/shell QDs based on CdSe cores and with different shell structures and number of shell monolayers; (B) Kinetic of CdSe/ZnS/CdS/ZnS QDs fluorescence quenching by different excess of AL.

Titration of QD solution with AL leads to PL quenching of all studied QDs. It can be seen that typical CdSe/ZnS QDs ( $d \sim 4.3$  nm) with a three-monolayer (3-ML) shell were completely quenched by addition of only 5 molar equivalents of acridine, whereas QDs with a “giant” (5-ML) ZnS shell ( $d \sim 7$  nm) and QDs with ZnS/CdS/ZnS “multishell” (MS) with a total shell thickness of 3-ML ( $d \sim 5$  nm) [30] exhibited a smaller degree of fluorescence quenching even, when the QD-to-acridine ratio reached 35. Thus, both MS and “giant” shell types provide more efficient protection of excited charge carriers in QDs from the quencher ligands than the “classic” thin ZnS shells. However, MS QDs are considerably smaller in physical size, which makes them more preferable as components of nanoprobes, since they could ensure better tissue and cell membrane penetration.

Charge transfer from QD to ligand molecules leads to positively or negatively charging of QD and, as a consequence, quenching of QD’s fluorescence. We suppose that in the studied system quenching is caused by electron transfer from QD to AL, because of the proximity of LUMO energy levels of both components. Schematic illustration of the photoinduced electron transfer (PET) mechanism from the core/shell QD to the AL is shown in Fig. 3. The LUMO level of AL is slightly lower than that of the CdSe core, which indicates that AL has favorable energetics for electron extraction from QD, which leads to charging of the QD and PL quenching. However, the probability of a PET process for

a different shell structures is different, since every different type of shell used in our experiments has its own barrier potential and length. In the case of a “classic” 3ML ZnS shell the barrier potential is sufficiently high to protect CdSe cores from environment, but fails to prevent PET when it is favorable, as in our case.

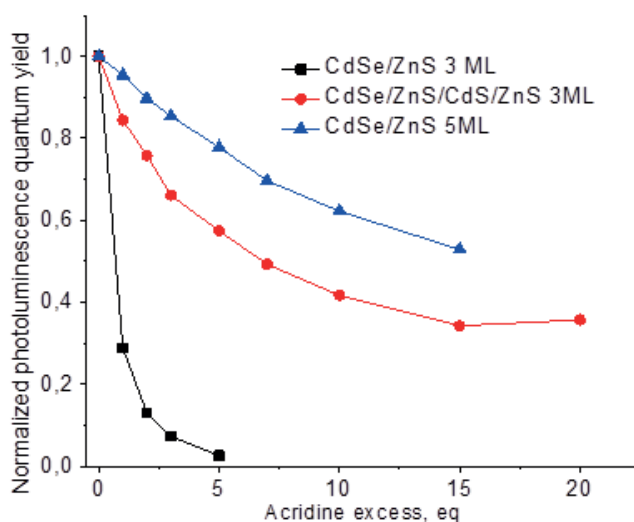


**Figure 2:** Kinetics of PL quenching of different QDs with increase of acridine ligand excess.

In 5ML “giant” ZnS shell the magnitude of the barrier can be considered the same, but, the tunneling length for the electron is higher. Thus, PET is much less effective in 5ML ZnS-shelled QDs. As for the “multishell” QDs, the quantum-confinement effect comes into place when the thickness of inner ZnS (and other two) layer is sufficiently thin, leading to an increase in the magnitude of confinement potential when compared to thick ZnS shell. As can be seen, our approach to engineering of confinement potential by creating a “multishell” structure allows to suppress PET with high efficiency.

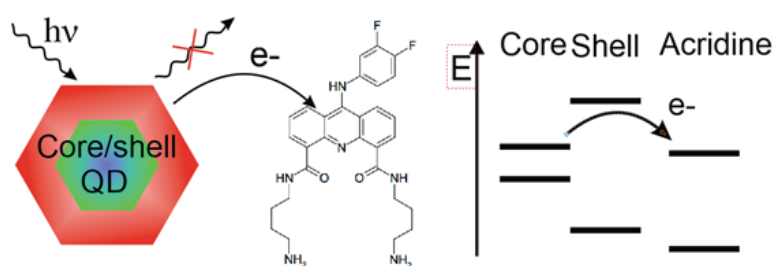


**Figure 3:** Schematic illustration of the photoinduced electron transfer mechanism from core/shell QD to the acridine ligand.

## 4. Results

In this work we demonstrate that structure of QD shells plays a key role in designing of acridine containing fluorescent nanoprobe. Our "multishell" (CdSe/ZnS/CdS/ZnS) QD structure provides a sufficient reduction of fluorescence quenching caused by PET, while maintaining a relatively small shell thickness. Thus, the core/multishell QDs could be an ideal choice for engineering of small-sized fluorescence labels for tumor diagnosis and treatment systems employing fluorescence quenching ligands capable of penetrating into cells and cellular compartments.

## Acknowledgments

This study was supported by the Russian Foundation for Basic Research (grant no. 16-34-60253) and by the University of Reims Champagne-Ardenne.

## References

- [1] Nagy A. et al. Comprehensive analysis of the effects of CdSe quantum dot size, surface charge, and functionalization on primary human lung cells. // *ACS nano*. 2012. Vol. 6, № 6. P. 4748–4762.
- [2] Shi J. et al. Nanotechnology in Drug Delivery and Tissue Engineering: From Discovery to Applications // *Nano Letters*. American Chemical Society, 2010. Vol. 10, № 9. P. 3223–3230.
- [3] Sukhanova A. et al. Oriented conjugates of single-domain antibodies and quantum dots: toward a new generation of ultrasmall diagnostic nanoprobe. // *Nanomedicine: nanotechnology, biology, and medicine*. 2012. Vol. 8, № 4. P. 516–525.
- [4] Bilan R. et al. Quantum Dot Surface Chemistry and Functionalization for Cell Targeting and Imaging // *Bioconjugate Chemistry*. 2015. Vol. 26, № 4. P. 609–624.
- [5] Linkov P. et al. Multifunctional Nanoprobe for Cancer Cell Targeting, Imaging and Anticancer Drug Delivery // *Physics Procedia*. 2015. Vol. 73. P. 216–220.
- [6] Samokhvalov P., Artemyev M., Nabiev I. Basic principles and current trends in colloidal synthesis of highly luminescent semiconductor nanocrystals. // *Chemistry - Eur. J.* 2013. Vol. 19, № 5. P. 1534–1546.
- [7] Dovzhenko D. et al. Enhancement of Spontaneous Emission from CdSe/CdS/ZnS Quantum Dots at the Edge of the Photonic Band Gap in a Porous Silicon Bragg Mirror

- // Physics Procedia. 2015. Vol. 73. P. 126–130.
- [8] Linkov P. et al. Ultrasmall Quantum Dots: A Tool for in Vitro and in Vivo Fluorescence Imaging // Journal of Physics: Conference Series. 2017. Vol. 784. P. 12033.
- [9] Zhao J.-Y. et al. Ultrasmall Magnetically Engineered Ag<sub>2</sub>Se Quantum Dots for Instant Efficient Labeling and Whole-Body High-Resolution Multimodal Real-Time Tracking of Cell-Derived Microvesicles // Journal of the American Chemical Society. 2016. Vol. 138, № 6. P. 1893–1903.
- [10] Wegner K.D., Hildebrandt N. Quantum dots: bright and versatile in vitro and in vivo fluorescence imaging biosensors // Chem. Soc. Rev. 2015. Vol. 44, № 14.
- [11] Sparapani S. et al. Rational design of acridine-based ligands with selectivity for human telomeric quadruplexes // Journal of the American Chemical Society. 2010. Vol. 132, № 35. P. 12263–12272.
- [12] Laronze-Cochard M. et al. Synthesis and biological evaluation of novel 4,5-bis(dialkylaminoalkyl)-substituted acridines as potent telomeric G-quadruplex ligands // European Journal of Medicinal Chemistry. 2009. Vol. 44, № 10. P. 3880–3888.
- [13] Burger A.M. The G-Quadruplex-Interactive Molecule BRACO-19 Inhibits Tumor Growth, Consistent with Telomere Targeting and Interference with Telomerase Function // Cancer Research. 2005. Vol. 65, № 4. P. 1489–1496.
- [14] Müller S. et al. Small-molecule-mediated G-quadruplex isolation from human cells // Nature Chemistry. Nature Research, 2010. Vol. 2, № 12. P. 1095–1098.
- [15] Artese A. et al. Toward the design of new DNA G-quadruplex ligands through rational analysis of polymorphism and binding data // European Journal of Medicinal Chemistry. 2013. Vol. 68. P. 139–149.
- [16] Cho A.-N. et al. Acridine-based novel hole transporting material for high efficiency perovskite solar cells // J. Mater. Chem. A. The Royal Society of Chemistry, 2017. Vol. 5, № 16. P. 7603–7611.
- [17] Krzymiński K. et al. <sup>1</sup>H and <sup>13</sup>C NMR spectra, structure and physicochemical features of phenyl acridine-9-carboxylates and 10-methyl-9-(phenoxy-carbonyl)acridinium trifluoromethanesulphonates – alkyl substituted in the phenyl fragment // Spectrochimica Acta Part A: Molecular and Biomolecular Spectroscopy. 2011. Vol. 78, № 1. P. 401–409.
- [18] Jasieniak J., Califano M., Watkins S.E. Size-Dependent Valence and Conduction Band-Edge Energies of Semiconductor Nanocrystals // ACS Nano. 2011. Vol. 5, № 7. P. 5888–5902.
- [19] Islam A. et al. Blue light-emitting devices based on 1,8-acridinedione derivatives // Synthetic Metals. 2003. Vol. 139, № 2. P. 347–353.

- [20] Liu I.-S. et al. Enhancing photoluminescence quenching and photoelectric properties of CdSe quantum dots with hole accepting ligands // *Journal of Materials Chemistry*. 2008. Vol. 18, № 6. P. 675.
- [21] Krivenkov V.A. et al. Surface ligands affect photoinduced modulation of the quantum dots optical performance // *SPIE Proceedings*. 2014. Vol. 9126. P. 91263N.
- [22] Bang J. et al. Photoswitchable quantum dots by controlling the photoinduced electron transfers // *Chemical Communications*. 2012. Vol. 48, № 73. P. 9174.
- [23] Linkov P. et al. Ultrasmall Quantum Dots for Fluorescent Bioimaging in vivo and in vitro // *Optics and Spectroscopy*. 2017. Vol. 122, № 1. P. 8–11.
- [24] Dubal D.P., Holze R. A successive ionic layer adsorption and reaction (SILAR) method to induce Mn<sub>3</sub>O<sub>4</sub> nanospots on CNTs for supercapacitors // *New Journal of Chemistry*. 2013. Vol. 37, № 2. P. 403.
- [25] Samokhvalov P. et al. Photoluminescence quantum yield of CdSe-ZnS/CdS/ZnS core-multishell quantum dots approaches 100
- [26] Chen Y. et al. "Giant" multishell CdSe nanocrystal quantum dots with suppressed blinking. // *Journal of the American Chemical Society*. 2008. Vol. 130, № 15. P. 5026–5027.
- [27] Razgoniaeva N. et al. One-dimensional carrier confinement in "giant" CdS / CdSe excitonic nanoshells. 2017.
- [28] Linkov P. et al. Comparative advantages and limitations of the basic metrology methods applied to the characterization of nanomaterials. // *Nanoscale*. 2013. Vol. 5, № 19. P. 8781–8798.
- [29] Jasieniak J. et al. Re-examination of the Size-Dependent Absorption Properties of CdSe Quantum Dots // *The Journal of Physical Chemistry C. American Chemical Society*, 2009. Vol. 113, № 45. P. 19468–19474.
- [30] Linkov P. et al. High Quantum Yield CdSe/ZnS/CdS/ZnS Multishell Quantum Dots for Biosensing and Optoelectronic Applications // *Materials Today: Proceedings*. 2016. Vol. 3, № 2. P. 104–108.